PHYSICAL REVIEW A VOLUME 22, NUMBER 3 SEPTEMBER 1980

Effects of intense magnetic and motional Stark fields on state mixing and transition line shapes

R. Panock,*† M. Rosenbluh, and B. Lax†
Francis Bitter National Magnet Laboratory, MIT, Cambridge, Massachusetts 02139

Terry A. Miller‡
Bell Laboratories, Murray Hill, New Jersey 07974
(Received 29 February 1980)

The theoretical treatment of the combined effects of strong magnetic and motional electric fields on a simple atom, such as ^{4}He, is developed. It is shown that normal selection rules are relaxed by the external fields and that many previously forbidden transitions become allowed. The transition moment is shown to be velocity dependent, resulting in new and unique line shapes for these transitions. The theory is presented in a form directly applicable to the experiments reported in the accompanying paper.

I. INTRODUCTION

In a previous work[1] we had reported our initial observations of normally "forbidden" transitions in ^{4}He. In this article we wish to give a detailed description of the breakdown of normal dipole selection rules due to the influence of an intense external magnetic field and the associated motional Stark field seen by the atom in its rest frame. We derive line shapes for such forbidden transitions for those conditions where the atomic velocity distribution is Maxwellian. In the following paper[2] experimental observations are presented which make full use of the theoretical treatment derived here. Since the object of this derivation is its applicability to our experimental results on ^{4}He, we will tend to present the theory in terms of the He Rydberg states. A generalization of the treatment to other systems is easily obtained from our results.

We will be concerned with three basically different situations. In one case the magnetic field is solely responsible for destroying normal selection rules by mixing states with the same parity ($\Delta L = \pm 2$), and m_L quantum number, via the diamagnetic term on the Zeeman Hamiltonian. This can lead, for example, to He transitions, such as $7\,^1S$-$9\,^1L$ ($L = 3, 5, 7$), ($m_L = \pm 1$). The second case involves the action of a motional Stark field which mixes states with $\Delta L = \pm 1$, and $\Delta m_L = \pm 1$. This leads to transitions such as $7\,^1S$-$9\,^1D$ ($m_L = \pm 2$). Finally we consider the case where both fields act together which leads to additional transitions such as $7\,^1S$-$9\,^1L$ ($L = 4, 6, 8$), ($m_L = \pm 2$).

For those cases where the selection rules are broken down by the motional Stark effect (MSE), which is velocity dependent, the atomic transition moments and saturation intensity will acquire a strong velocity dependence. A line-shape derivation for such transitions therefore has to include both the MSE shift of the atomic energies and the MSE-dependent transition moment and saturation intensity prior to the integration over the velocity distribution. For the case where the magnetic field is solely responsible for breaking down the selection rules, the line shape is the same as that derived previously[3,4] which includes only the MSE-dependent shift of the atomic energies.

II. ATOMIC EIGENVALUES AND VECTORS IN AN INTENSE MAGNETIC FIELD

For the purposes of the present study the effect of an intense external magnetic field on an atomic system is threefold. (1) It directly alters the energies of the atomic levels via the well known linear and diamagnetic Zeeman effects.[5,6] This permits, for example, the tuning of atomic energy levels into resonance with the fixed frequency of a laser. (2) The magnetic field, via the diamagnetic term, mixes various states, in turn modifying the normal spectroscopic selection rules. (3) The magnetic field engenders a motional electric field which is proportional to the magnetic field and the component of atomic motion perpendicular to the magnetic field. This motional Stark field further alters the atomic energies and the spectroscopic selection rules.

Fortunately the variation of the atomic energies due to the MSE is small compared to the terms of the Zeeman Hamiltonian. Thus, we can solve the problem in two stages. First we obtain the eigenvalues and eigenvectors, neglecting the motional Stark field. We then take the MSE into account using perturbation theory.

We make several approximations in our choice of a basis set. For moderately high Rydberg states, the separation between levels differing in

the principle quantum number n, is still very large compared to the Hamiltonian terms involving the external fields, which connect them. Thus we consider only an isolated n manifold and neglect coupling between n states.

The states in a specific n manifold can again be subdivided according to whether they are singlet or triplet states. For states with large angular momentum $\vec{L}$ it is known that the electron spin $\vec{S}$ is not well conserved. However, at the large magnetic fields we are concerned with $\vec{L}$ and $\vec{S}$ are completely decoupled and the states mixed by the spin-orbit coupling are now tuned far apart.[7] Therefore we can consider singlet and triplet states separately. A slight difficulty is encountered in such a treatment when extrapolating to the zero-field energies, but this is easily dealt with for any given set of states. The corrections needed for the He spectra, for example, are outlined in Sec. IV D of the following paper.

In general, the matrix elements needed to construct the relevant Hamiltonian are well approximated using hydrogenic wave functions. However, for the accuracy required in the present studies, n must always be replaced by n^* (using the generally known quantum defect), and the off-diagonal Zeeman matrix elements actually used were computed by numerical integration using a computer program written by M. Zimmerman.[8]

A. The complete Zeeman Hamiltonian

The Hamiltonian for a stationary atom in an external magnetic field, $\vec{B}$, is given by

$$\hat{\mathcal{H}}=\hat{\mathcal{H}}_0+u_0 g_L \vec{B}\cdot\vec{L}+\sum_i \frac{e^2}{8mc^2} B^2 r_i^2 \sin^2\theta_i , \qquad (1)$$

where the symbols have their usual significance.[1] The indicated coordinates are summed over all electrons, but by far the dominant contribution and the only one that changes in transitions, such as those described in the following paper, comes from the Rydberg electron. The g_L is the orbital g factor; it is well approximated by $g_L = 1 - m/M$, which for ^{4}He gives $g_L = 0.999\,86$. $\hat{\mathcal{H}}_0$ is the zero-field Hamiltonian which reproduces the actual (non-hydrogenic) energy levels of the n, L states of the atom.

The second term of $\hat{\mathcal{H}}$ is completely diagonal in the spherically symmetric basis set of the eigenfunctions of $\hat{\mathcal{H}}_0$, and gives rise to the normal linear Zeeman effect, $g_L u_0 B m_L$. The last term of $\hat{\mathcal{H}}$ represents the diamagnetic Zeeman interaction.[9] It has diagonal matrix elements in the eigenfunction basis, but it also has elements connecting states with $\Delta L = \pm 2$, $\Delta m_L = 0$. If we include only the Rydberg electron, the matrix elements for the last term are

$$\frac{e^2B^2}{8mc^2}\langle n, L, m_L | r^2\sin^2\theta | n, L, m_L\rangle = \frac{e^2B^2}{4mc^2}\left(\frac{L(L+1)+m_L^2-1}{(2L+3)(2L-1)}\right) \times \{\tfrac{1}{2}n^2a_0^2[5n^2+1-3L(L+1)]\} \quad (2a)$$

and

$$\frac{e^2B^2}{8mc^2}\langle n, L, m_L | r^2\sin^2\theta | n, L-2, m_L\rangle = -\frac{e^2B^2}{8mc^2}\left(\frac{(L^2-M_L^2)[(L-1)^2-M_L^2]}{(2L+1)(2L-1)^2(2L-3)}\right)^{1/2} \times \{\tfrac{5}{2}n^2a_0^2[(n^2-(L-1)^2)(n^2-L^2)]^{1/2}\}, \quad (2b)$$

with the matrix elements for $L' = L+2$ being trivially obtained from the above. In both equations the portion in curly brackets represents the integral of r^2 over hydrogenic wave functions. While this is a good approximation (especially if we substitute n^* for n in the diagonal element), a more precise result is obtained by numerically evaluating r^2 using, for example, the computer code of Zimmerman[8] and using this calculated value in place of the expression in curly brackets.

The matrix elements of the Hamiltonian, Eq. (1), are seen not to connect even L states with odd L states as required by parity conservation. Similarly the matrix is diagonal in the magnetic quantum number m_L as required by the cylindrical symmetry of the problem. Thus to solve the Zeeman problem we have to diagonalize a matrix consisting of either all odd, or all even, parity states of a given n and m_L. Besides eigenvalues we also obtain eigenvectors describing the "perturbed" states, particularly their angular composition. While these states can actually be quite mixed we will identify them by their angular momentum quantum number in zero field, L_0, obtained in the adiabatic limit, and their "good" quantum numbers, n and m_L, i.e.,

$$|L_0, m_L, n\rangle = \sum_L C(L_0, m_L, L)|L, m_L, n\rangle . \qquad (3)$$

B. The effects of the motional electric field

In Sec. II A we wrote down the complete Zeeman Hamiltonian for a stationary atom in the magnetic field. In practice, however, the atoms are moving in a static magnetic field and the interaction of this motion and the magnetic field produces an effective electron field, F, at the atom given by[3]

$$F = (\vec{v}\times\vec{B})/c = Bv_\perp/c , \qquad (4)$$

where $v_\perp$ is the component of the atom's velocity

perpendicular to the magnetic field. The effect of this motional Stark field, F, is twofold. It changes the energies of the new states, $|L_0, m_L, n\rangle$ and perturbs their wave functions by mixing even- and odd-parity states. Fortunately these effects are generally small enough to be adequately treated by perturbation theory. The corrected energy E_2 is related to the eigenvalue associated with $|L_0, m_L, n\rangle$ by

$$E_2 = E(L_0) - \tfrac{1}{2}\alpha_L F_\perp^2 , \tag{5}$$

where α_L is the polarizability associated with the state $|L_0, m_L, n\rangle$. Although not explicitly shown, α_L is a function of the magnetic field. In a similar way we obtain a corrected wave function, $|L_0, m_L, n, 2\rangle$,

$$\begin{aligned} &|L_0, m_L, n, 2\rangle \\ &= |L_0, m_L, n\rangle + \sum_{k(\neq i)} \frac{H_{ik}}{E_i(L_0) - E_k(L_0)} |L_0^k, m_L \pm 1, n\rangle \\ &= |L_0, m_L, n\rangle + \sum_{k(\neq i)} Q_{ik} |L_0^k, m_L \pm 1, n\rangle , \end{aligned} \tag{6}$$

where

$$H_{ik} = \langle L_0^i, m_L, n | e\vec{F}\cdot\vec{r} | L_0^k, m_L, n\rangle \tag{7}$$

is the matrix element of the motional Stark perturbation, H_F, between the eigenfunction states, $|L_0, m_L, n\rangle$.

Equations (5) and (6) give compact expressions for the effect of the motional electric field on the energies and eigenfunctions. Unfortunately, they contain polarizabilities and other matrix elements evaluated for the states $|L_0, m_L, n\rangle$, whereas it is convenient to calculate these quantities using the basis states $|L, m_L, n\rangle$. To obtain the matrix elements governing the perturbed wave functions we expand Eq. (7) using Eq. (3),

$$\begin{aligned} H_{ik} = \sum_{L^i, L^k} \sum_{m_L} & C^*(L_0^i, m_L, L^i) C(L_0^k, m_L', L^k) \\ & \times \langle L^i, m_L, n | H_F | L^k, m_L', n\rangle . \end{aligned} \tag{8}$$

The matrix elements of H_F in the above equation are to a very good approximation just those of the vector $\vec{r}$ (times a constant) for hydrogenic wave functions. These are obtained from Condon and Shortley[9] and given in Table I for reference. From these matrix elements it is clear that H_{ik} is nonzero only if $m_L' = m_L \pm 1$ and $L^k = L^i \pm 1$. In a similar way we can find an explicit expression for α_L in terms of the matrix elements H_{ik}, given in Eq. (8),

$$\alpha_L^i = \frac{-2}{F_\perp^2} \sum_{k(\neq i)} \frac{|H_{ik}|^2}{E_i(L_0) - E_k(L_0)} . \tag{9}$$

It may be noted that this expression reduces to that given for the definition of α' in Eq. (13) of Ref. 4 if $C(L_0, m_L, L) = \delta_{L_0, L}$, a sufficiently accurate approximation for the observations reported there.

III. LINE-SHAPE ANALYSIS

There are two fundamentally different contributions to an atomic transition line shape: velocity independent and velocity dependent. In Ref. 4 we outlined a general method of obtaining atomic resonance line shapes. The derivation starts with the Lorentzian response function for a single velocity group of atoms. Provided that one is concerned with a thermal distribution of atoms the next step is to average the Lorentzian over a

TABLE I. Matrix elements of electric field Hamiltonian, $\hat{\mathcal{H}}_F$, evaluated for hydrogenic basis functions, $|L, m_L, n\rangle$.

$$\langle L, m_L, n | \hat{\mathcal{H}}_F | L', m_L', n\rangle = \delta_{L', L+1}\delta_{m_L', m_L+1} \tfrac{3}{4} n a_0 e \times (F_x - iF_y) \left(\frac{[n^2 - (L+1)^2](L + m_L + 1)(L + m_L + 2)}{(2L+1)(2L+3)} \right)^{1/2}$$

$$\langle L_1 m_L, n | \hat{\mathcal{H}}_F | L', m_L', n\rangle = -\delta_{L', L-1}\delta_{m_L', m_L+1} \tfrac{3}{4} n a_0 e \times (F_x - iF_y) \left(\frac{(n^2 - L^2)(L - m_L)(L - m_L - 1)}{(2L+1)(2L+3)} \right)^{1/2}$$

$$\langle L, m_L, n | \hat{\mathcal{H}}_F | L' 1 m_L', n\rangle = -\delta_{L', L+1}\delta_{m_L', m_L-1} \tfrac{3}{4} n a_0 e \times (F_x + iF_y) \left(\frac{[n^2 - (L+1)^2](L - m_L + 1)(L - m_L + 2)}{(2L+1)(2L+3)} \right)^{1/2}$$

$$\langle L_1 m_L, n | \hat{\mathcal{H}}_F | L', m_L', n\rangle = \delta_{L', L-1}\delta_{m_L', m_L-1} \tfrac{3}{4} n a_0 e \times (F_x + iF_y) \left(\frac{(n^2 - L^2)(L + m_L)(L + m_L - 1)}{(2L+1)(2L-1)} \right)^{1/2}$$

Maxwell-Boltzmann distribution of velocities. In the absence of external fields, this procedure yields the well known Voigt profile. In the presence of an intense external magnetic field, however, the atomic resonance frequency is not only Doppler shifted but can also undergo a shift due to the presence of the motional Stark field seen by the atom in its rest frame. This motional Stark field-induced frequency shift is velocity dependent, and to obtain the correct line shape it has to be included into the Lorentzian response function prior to the integration over the velocity distribution.

Such a derivation was performed in Ref. 4, and resulted in our ability to understand and fit the asymmetric line shape observed in the $7\,^1S$-$9\,^1P$ transitions. The line shape derived there, [Eq. (11)] is also applicable in the case of the forbidden transitions where the mixing of states that leads to their nonzero oscillator strength takes place solely through the diamagnetic term in the Hamiltonian. It is, therefore, velocity independent and does not enter into the line-shape analysis. Such transitions, from the $7\,^1S$ state to $n=9$ odd-parity states in He are described in the following paper.

For those forbidden transitions in which the mixing of states occurs via the MSE however, the transition moment (oscillator strength) is also velocity dependent.[1] Examples of such transitions will be seen in the following paper between the $7\,^1S$ and $9\,^1D$ ($m_L=\pm 2$) states, for example. Since slowly moving atoms will have transition moments much smaller than those with large speeds perpendicular to the magnetic field, the laser intensity required to saturate the transition (saturation intensity) will also be velocity dependent. In fact some atoms (those moving with extremely high speeds) will be saturated even at very low laser intensities. Furthermore, we shall see that the velocity-dependent transition moment and saturation intensity can be very significant even in cases where the motional Stark shift of the resonance frequency is negligible. Thus the line shape derivation also has to take these effects into account prior to the integration over the velocity distribution.

The mathematical manipulations used in arriving at such a transition line shape are tedious and somewhat similar to the methods used in Ref. 4. We present the derivation in the appendix. In the following discussion we will highlight the results of the derivation and concentrate on their physical interpretation.

A. Line shape with velocity dependent transition moment

1. The line-shape function

We start with the Lorentzian response function for an atom at rest with a transition resonance frequency at ν_0. If we let $f(\nu)$ represent the fractional decrease in the population of atoms in some lower state, when a laser with intensity I and frequency ν is incident on them, we find[10,11]

$$f(\nu)=\frac{I}{I_s}\frac{\Delta N_0}{N_{10}}\frac{\tau_1}{\tau_1+\tau_2}\frac{(\Gamma/2)^2}{(\nu-\nu_0)^2+(\Gamma/2)^2(1+I/I_s)}, \tag{10}$$

where the saturation intensity, I_s, is given by

$$I_s=\hbar^2 c/4\pi\mu_{12}^2 T_2(\tau_1+\tau_2), \tag{11}$$

and ΔN_0 is the difference in initial population densities in the lower and upper states, τ_1 and τ_2 are the characteristic lifetimes of the lower and upper states, respectively, μ_{12} is the dipole moment for the transition. The phase coherence time or the decay constant of the induced dipole is T_2 (given by $1/T_2=1/\tau_1+1/\tau_{\text{elastic collisions}}$),[12] and $\Gamma\equiv 1/\pi T_2$ is the full width at half maximum for the unsaturated line shape.

For an atom in motion in a magnetic field, Eqs. (10) and (11) have to be modified. First the resonance term, $(\nu-\nu_0)^2$ in Eq. (10) is replaced by

$$\left(\nu-\nu_0-\frac{v_y\nu_0}{c}+\frac{1}{2}\frac{\alpha_L}{h}\frac{v_\perp^2}{c^2}B^2\right)^2,$$

where y is the direction of laser propagation, $v_\perp$ is the velocity in the xy plane perpendicular to the magnetic field B defining the z axis, and α_L is the previously defined polarizability of the atom. The modification consists of redefining I_s in Eq. (11) so as to make it a velocity-dependent quantity. Therefore we replace I_s by $I_{s0}v_0^2/v_\perp^2$ where I_{s0} is given by

$$I_{s0}=\hbar^2 c/8\pi M_{um}^0\mu_{lm}^2 T_2\tau, \tag{12}$$

v_0 is the thermal velocity, μ_{lm} is the dipole moment for the normally allowed transition from the lower state l to some state m, and $M_{um}^{(0)}$ is the square of the mixing coefficient between the upper state u and the lower state m for an atom with $v_\perp=v_0$, as defined by Eq. (6), i.e.,

$$M_{um}^0=|Q_{um}|^2. \tag{13}$$

With these additions and changes, and including the integration over a Maxwell-Boltzmann velocity distribution, we obtain for our line-shape function:

$$f(\nu)=\frac{1}{\pi v_0^2}\frac{I}{I_{s0}}\frac{\tau_1}{\tau_1+\tau_2}\frac{\Delta N_0}{N_{10}}\left(\frac{\Gamma}{2}\right)^2\int\int_{-\infty}^{\infty}\frac{(v_\perp^2/v_0^2)\exp(-v_\perp^2/v_0^2)}{[\Delta\nu-v_y\nu_0/c+\frac{1}{2}(\alpha v_\perp^2/hc^2)B^2]^2+(\Gamma/2)^2[1+(I/I_{s0})(v_\perp^2/v_0^2)]}\,dv_x dv_y, \tag{14}$$

which has recently been given in Ref. 1.

The general line shape represented by the above equation is not an exact integral and in its present form is not easy to physically interpret. By examining some limiting cases however, we can get a physically meaningful picture of the line shape. We will consider Eq. (14) under three conditions: (a) no saturation—large MSE, (b) no saturation—small MSE, and (c) saturation—large MSE. The case of saturation with small MSE will not be examined since it is experimentally hard to achieve saturation in those cases where the MSE and thus the mixing is small.

2. *No saturation—large MSE*

Using the results of the Appendix [see Eq. (A9)] and the definitions of γ, γ_H, and γ_D, we obtain that when $\gamma_D \to 0$ and

$$1+(I/I_{SO})(v_1^2/v_0^2)\to 1$$

and $\gamma_H \ll 1$,

$$f(\nu)=\begin{cases} 0, & \gamma \geq 0 \\ -\dfrac{I}{I_{SO}}\dfrac{\tau_1}{\tau_1+\tau_2}\dfrac{\Delta N_0}{N_{10}}\dfrac{\gamma_H}{2}\gamma e^{\gamma}, & \gamma<0. \end{cases} \tag{15}$$

(γ_1, γ_H, and γ_D physically are the frequency offset from line center in units of the MSE shift for an atom with perpendicular speed v_0; the ratio of the homogeneous width to the MSE shift for a v_0 atom; the ratio of the Doppler shift to the MSE shift for a v_0 atom, respectively). We again observe the same type of cutoff behavior as we did in Ref. 3 for the allowed transitions. There is, however, one important difference, i.e., here at the cutoff the value of the line shape is zero. The reason for this is quite simple: The only atoms able to undergo a transition at line center ($\gamma=0$) are those atoms with zero perpendicular velocity. These atoms, however, have no transition moment and are thus unable to make the transition. As one moves away from line center the signal strength increases due to the concurrent increase in the perpendicular speeds of the atoms, which results in larger oscillator strengths. The signal does not increase continuously of course. At some point the number of atoms with large perpendicular speeds begins to drastically decrease and this decreasing population dominates over the increasing transition moment. The function $-\gamma e^{+\gamma}$ ($\gamma<0$) actually reaches a maximum when $\gamma=-1$ which implies that the line shape has a maximum value at a frequency offset from line center, $\Delta\nu$, equal to the MSE-induced shift in the atomic resonance frequency for a $v_\perp = v_0$ atom. An example of this type of line shape is shown in Fig. 1.

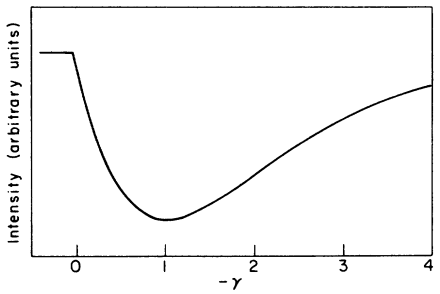

FIG. 1. Illustration of the line shape, $+\gamma e^{-\gamma}$, which is applicable when the MSE dominates over both the Doppler effect and homogeneous broadening mechanisms.

3. *No saturation—small MSE*

Although a small MSE also implies very small mixing coefficients and thus oscillator strengths, forbidden transitions with almost negligible MSE are still observable, provided enough laser power is available to drive the transition. In fact many of the observed transitions to the He even-parity states fall into this category.[2] To arrive at a line shape for this case we define the quantity q to be the ratio of the homogeneous half width at half maximum to the Doppler half width at $\frac{1}{2}$max, and assume that $q \ll 1$ and that $\alpha_L \to 0$. We then get [see Eq. (A15)]

$$f(\nu)=\sqrt{\pi}\,\frac{I}{I_{SO}}\,\frac{\tau_1}{\tau_1+\tau_2}\,\frac{\Delta N_0}{N_{10}}\,q(\tfrac{1}{2}+\delta^2)e^{-\delta^2}, \tag{16}$$

where

$$\delta=\Delta\nu c/\nu_0 v_0.$$

This line shape is illustrated in Fig. 2.

The most obvious feature of this line shape is the dip at line center. This is again due to the fact that at line center, atoms are generally mov-

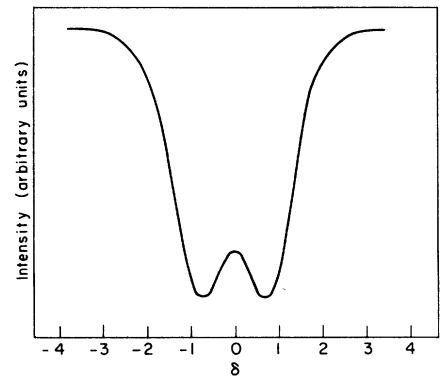

FIG. 2. Illustration of the line shape, $(\frac{1}{2}+\delta^2)e^{-\delta^2}$, which is applicable when the MSE is negligible and the homogeneous width is small compared to the Doppler width.

ing slower and therefore have a reduced transition moment. The reason that the signal does not go to zero at line center is that the atoms contributing signal must have $v_y = 0$ (no Doppler shift) but they can have an arbitrary v_x, which provides them with some oscillator strength. As one moves off line center to nonzero v_y values (and still arbitrary v_x) the transition moment and therefore the signal increase. Of course, as v_y (and therefore Δv) gets larger there are fewer atoms and the decrease in the number of atoms again overcomes the increasing transition moment resulting in an overall decrease in signal. It turns out that the full width half maximum (FWHM) for this line shape corresponds to a $\Delta\delta \approx 3$, which is almost a factor of 2 larger than for a normal, Doppler-broadened, line.

4. *Saturation—large MSE*

When saturation effects are included into the line shape, the clearly resonant behavior in the denominator of the integrand in Eq. (14) is lost as the width for each perpendicular velocity group becomes different. We are in fact able to transform this rather complicated looking two-dimensional integral into a one-dimensional integral [as given by Eqs. (A19) and (A20)]. This transformation does not aid greatly in the physical interpretation of the line-shape equation, but it is useful in the numerical analysis of data.

The most noticeable effect of saturation occurs when the MSE is very large in comparison to the Doppler effect. In this limit the frequency (or field) at which an atom absorbs or emits a photon is directly determined by the atom's perpendicular velocity. As already pointed out, atoms contributing to the signal near line center are moving very slowly ($v_\perp < v_0$) while atoms contributing to signal on the "tail" are moving very fast ($v_\perp > v_0$). Thus at a given laser intensity slow atoms are not near saturation while there are always some fast atoms for which the transition is saturated. When one increases the laser intensity, slow-moving atoms can have a proportional increase in signal strength while fast atoms, because they are nearly saturated, cannot. This has the effect then of a narrowing of the spectral linewidth. This is quite unusual in that saturation is usually associated with spectral line broadening. This behavior is shown in Fig. 3, which for illustrative purposes was made by assuming a rather large value for q, the ratio of the power-broadened homogeneous width to the Doppler width. Saturation effects do tend to narrow the observed lines and must be included in the line-shape analysis of the data presented in the following paper.

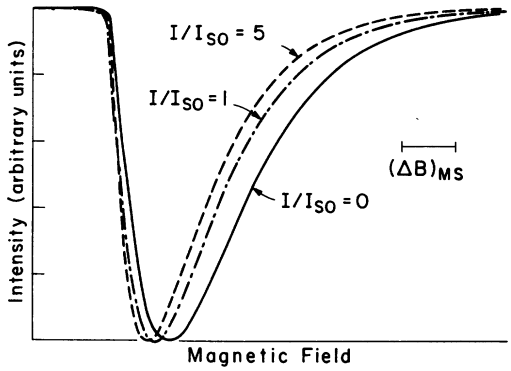

FIG. 3. The effect of saturation on a spectral line for which the MSE dominates the Doppler effect. In this figure the Doppler shift is assumed to be zero, and the ratio of the homogeneous width (FWHM) to the motional Stark shift (for a $v_\perp = v_0$ atom) is assumed to be 0.029.

The effect of saturation is comparatively small when the MSE is very small. For reasonable laser intensities and lifetimes of states the effect of saturation is to "wash out" the structure in the spectral line. For large laser intensities, the line can become narrower near the peak and wider at the base of the line.

IV. CONCLUSION

In this paper we have presented a general method for dealing with the full Zeeman Hamiltonian. The method is applicable to all cases and its only eventual limitation is the size of the matrix that one needs to diagonalize. In addition we have shown how through the use of perturbation theory, one can include the effects of motional Stark fields. Line shapes were derived for transitions to magnetically and electrically (MSE) mixed states. These line shapes are unique in that they have included in them a velocity-dependent transition moment, saturation intensity and energy resonance term. The theory is developed in a form directly applicable to our experimental observations reported in the following paper.

ACKNOWLEDGMENT

The work of R. P., M. R., and B. L. was supported by the National Science Foundation.

APPENDIX: LINE-SHAPE CALCULATIONS

In this appendix, we evaluate the integral in Eq. (14) both in simplifying circumstances and with no approximation. Although the integral can be reduced in general to a one-dimensional integral, the value of treating it under simplifying assumptions is that we obtain a clear understanding of the line-shape function.

A. Ignore saturation effects

We first neglect the effect of saturation. Making the substitutions,

$$u_x = v_x/v_0, \quad u_y = v_y/v_0,$$

$$\gamma = \frac{\Delta\nu}{\frac{1}{2}(\alpha/h)(v_0^2/c^2)B^2}, \quad \gamma_D = \frac{(v_0/c)\nu_0}{\frac{1}{2}(\alpha/h)(v_0^2/c^2)B^2}, \quad \gamma_H = \frac{\Gamma}{\frac{1}{2}(\alpha/h)(v_0^2/c^2)B^2},$$

and setting $I/I_{SO} = 0$ in the denominator, we obtain

$$f(\gamma) = \frac{1}{\pi}\frac{I}{I_{SO}}\frac{\tau_1}{\tau_1+\tau_2}\frac{\Delta N_0}{N_{10}}\left(\frac{\gamma_H}{2}\right)^2 \int\int_{-\infty}^{\infty} du_x du_y \frac{(u_x^2+u_y^2)e^{-(u_x^2+u_y^2)}}{(\gamma-\gamma_D u_x+u_x^2+u_y^2)^2+(\gamma_H/2)^2}. \tag{A1}$$

Substituting

$$w = u_x - \tfrac{1}{2}\gamma_D,$$

we obtain

$$f(\nu) = \frac{1}{\pi}\frac{I}{I_{SO}}\frac{\tau_1}{\tau_1+\tau_2}\left(\frac{\gamma_H}{2}\right)^2 \int\int_{-\infty}^{\infty} dw\, du \frac{(w^2+u^2+\frac{1}{4}\gamma_D^2+\gamma_D w)e^{-(u^2+w^2+\gamma_D w+(1/4)\gamma_D^2)}}{(a^2+u^2+w^2)^2+(\gamma_H/2)^2}, \tag{A2}$$

where $a^2 = \gamma - \frac{1}{4}\gamma_D^2$.

Converting to polar coordinates:

$$u = z\sin\theta, \quad w = z\cos\theta,$$

$$f(\nu) = \frac{1}{\pi}\frac{I}{I_{SO}}\frac{\tau_1}{\tau_1+\tau_2}\frac{\Delta N_0}{N_{10}}\left(\frac{\gamma_H}{2}\right)^2 e^{-\gamma_D^2/4}\int_0^{2\pi} d\theta \int_0^{\infty} z\, dz \frac{(z^2+\frac{1}{4}\gamma_D^2+\gamma_D z\cos\theta)e^{-z^2}e^{-\gamma_D z\cos\theta}}{(a^2+z^2)^2+(\gamma_H/2)^2}. \tag{A3}$$

Using the identify

$$I_0(x) = \frac{1}{2\pi}\int_0^{2\pi} d\theta\, e^{x\cos\theta} = \frac{1}{2\pi}\int_0^{2\pi} d\theta\, e^{-x\cos\theta}, \tag{A4}$$

and the additional identity

$$I_1(x) = I_0'(x) = -\frac{1}{2\pi}\int_0^{2\pi} \cos\theta\, e^{-x\cos\theta} d\theta, \tag{A5}$$

we get

$$f(\nu) = 2\frac{I}{I_{SO}}\frac{\tau_1}{\tau_1+\tau_2}\frac{\Delta N_0}{N_{10}}\left(\frac{\gamma_H}{2}\right)^2 e^{-\gamma_D^2/4}\int_0^{\infty} z\, dz \frac{(z^2+\frac{1}{4}\gamma_D^2)I_0(\gamma_D z)-\gamma_D z I_1(\gamma_D z)}{(a^2+z^2)^2+(\gamma_H/2)^2}e^{-z^2}, \tag{A6}$$

and with

$$x = z^2, \quad x_0 = -a^2 = \tfrac{1}{4}\gamma_D^2 - \gamma,$$

we obtain

$$f(\nu) = \frac{I}{I_{SO}}\frac{\tau_1}{\tau_1+\tau_2}\frac{\Delta N_0}{N_{10}}\left(\frac{\gamma_H}{2}\right)^2 e^{\gamma-\gamma_D^2/2}\int_{-x_0}^{\infty} dy \frac{(y+x_0+\frac{1}{4}\gamma_D^2)I_0[\gamma_0(y+x_0)^{1/2}]-\gamma_D(y+x_0)^{1/2}I_1[\gamma_D(y-x_0)^{1/2}]}{y^2+(\gamma_H/2)^2}. \tag{A7}$$

From the above formula it is still rather difficult to discern easily the properties of the line shape, therefore we consider two limiting cases: (1) large MSE, (2) no MSE.

1. Velocity-dependent transition moment: Large MSE

We examine Eq. (A7) in the limit $\gamma_D \to 0$. In this limit $I_0[\gamma_D(y+x_0)^{1/2}] \to 0$, thus we obtain

$$f(\nu) = \frac{I}{I_{SO}}\frac{\tau_1}{\tau_1+\tau_2}\frac{\Delta N_0}{N_{10}}\left(\frac{\gamma_H}{2}\right)^2 e^{\gamma}\int_{\gamma}^{\infty}\frac{(y-\gamma)e^{-\gamma}}{y^2+(\gamma_H/2)^2}\,dy. \tag{A8}$$

Furthermore, for very large MSE $\gamma_H \ll 1$, and we obtain

$$f(\nu)=\begin{cases} 0, & \gamma>0 \\ -\dfrac{I}{I_{SO}}\dfrac{\tau_1}{\tau_1+\tau_2}\dfrac{\Delta N_0}{N_{10}}\dfrac{\gamma_H}{2}\gamma e^{\gamma}, & \gamma<0. \end{cases} \tag{A9}$$

2. Velocity-dependent transition moment: No MSE

To calculate the line shape when the MSE goes to zero we start with Eq. (14) and set α (and I/I_{SO} in the denominator) equal to zero. [We could have started with Eq. (A7) and calculated the Bessel function in the limit of very large argument but it is simpler to start from the beginning.] Thus when $\alpha \to 0$ the line-shape function becomes

$$f(\nu)=\frac{1}{\pi v_0^2}\frac{I}{I_{SO}}\frac{\tau_1}{\tau_1+\tau_2}\frac{\Delta N_0}{N_{10}}\left(\frac{\Gamma}{2}\right)^2\int\int_{-\infty}^{\infty} dv_x dv_y \frac{(v_1^2/v_0^2)e^{-(v_1^2)/v_0^2}}{[\Delta\nu-(v_y/c)\nu_0]^2+(\Gamma/2)^2}. \tag{A10}$$

Defining

$$u=v_y/v_0,\quad w=v_x/v_0,\quad \delta=\Delta\nu c/\nu_0 v_0,\quad q=(c/\nu_0 v_0)\Gamma/2, \tag{A11}$$

we obtain

$$f(\nu)=\frac{1}{\pi}\frac{I}{I_{SO}}\frac{\tau_1}{\tau_1+\tau_2}\frac{\Delta N_0}{N_{10}}q^2\int\int_{-\infty}^{\infty} du\,dw\,\frac{(u^2+w^2)e^{-(u^2+w^2)}}{(\delta-w)^2+q^2}; \tag{A12}$$

using the relations

$$\int_{-\infty}^{\infty} e^{-u^2}du=\sqrt{\pi},\qquad \int_{-\infty}^{\infty} u^2e^{-u^2}du=\frac{\sqrt{\pi}}{2}, \tag{A13}$$

we obtain

$$f(\nu)=\frac{1}{\sqrt{\pi}}\frac{I}{I_{SO}}\frac{\tau_1}{\tau_1+\tau_2}\frac{\Delta N_0}{N_{10}}q^2\int_{-\infty}^{\infty} dw\,\frac{(\frac{1}{2}+w^2)e^{-w^2}}{(\delta-w)^2+q^2}. \tag{A14}$$

If q (the ratio of the homogeneous half width at half maximum to the Doppler half width at $(1/e)$ max) is $\ll 1$, then we get

$$f(\nu)=\sqrt{\pi}\frac{I}{I_{SO}}\frac{\tau_1}{\tau_1+\tau_2}\frac{\Delta N_0}{N_{10}}q(\tfrac{1}{2}+\delta^2)e^{-\delta^2}. \tag{A15}$$

B. Inclusion of saturation

We now evaluate the integral in Eq. (14) with no simplifying approximations. We make the substitutions $v_x=-uv_0\cos\theta$, $v_y=uv_0\sin\theta$,

$$\delta=\frac{\Delta\nu c}{\nu_0 v_0},\quad q=\frac{\Gamma}{2}\frac{c}{\nu_0 v_0},\quad \delta_{MSE}=\frac{1}{2}\frac{\alpha}{h}\cdot\frac{B^2 v_0}{c\nu_0}\left(=\frac{\Delta\nu_{MSE}}{\Delta\nu_{DOP}}\right), \tag{A16}$$

Eq. (14) becomes

$$f(\nu)=\frac{1}{\pi}\frac{I}{I_{SO}}\frac{\tau_1}{\tau_1+\tau_2}\frac{\Delta N_0}{N_{10}}q^2\int_0^{\infty} du\,u^3e^{-u^2}\int_0^{2\pi} d\theta\,\frac{1}{[(\delta+\delta_{MSE}u^2)-u\cos\theta]^2+q^2[1+(I/I_{SO})u^2]}. \tag{A17}$$

Defining $\delta'=\delta+\delta_{MSE}u^2$, $q'=q[1+(I/I_{SO})u^2]^{1/2}$, we get

$$f(\nu)=\frac{1}{\pi}\frac{I}{I_{SO}}\frac{\tau_1}{\tau_1+\tau_2}\frac{\Delta N_0}{N_{10}}q^2\int_0^{\infty} du\,u^3e^{-u^2}\int_0^{\infty} d\theta\,\frac{1}{(\delta'-u\cos\theta)^2+(q')^2}. \tag{A18}$$

The above polar integral is calculable (Ref. 10) and we can write

$$f(\nu)=\sqrt{2}\frac{I}{I_{SO}}\frac{\tau_1}{\tau_1+\tau_2}\frac{\Delta N_0}{N_{10}}q\int_0^{\infty} du\,u^3e^{-u^2}I'(u), \tag{A19}$$

where

$$I'(u)=\left(\frac{[(\delta'^2-q'^2-u^2)^2+4q'^2\delta'^2]^{1/2}-(\delta'^2-q'^2-u^2)}{(\delta'^2-q'^2-u^2)^2+4q'^2\delta'^2}\right)^{1/2}. \tag{A20}$$

*Present address: Bell Laboratories, Holmdel, New Jersey 07733.
†Also, Physics Dept., MIT.
‡Guest at the Francis Bitter National Magnet Lab.

[1]R. Panock, M. Rosenbluh, B. Lax, and T. A. Miller, Phys. Rev. Lett. 42, 172 (1979).
[2]R. Panock, M. Rosenbluh, B. Lax, and T. A. Miller, Phys. Rev. A 22, 1050 (1980).
[3]M. Rosenbluh, T. A. Miller, D. M. Larson, and B. Lax, Phys. Rev. Lett. 39, 874 (1977).
[4]M. Rosenbluh, R. Panock, B. Lax, and T. A. Miller, Phys. Rev. A 18, 1103 (1978).
[5]F. A. Jenkins and E. Segre, Phys. Rev. 55, 52 (1939).
[6]L. I. Schiff and H. Snyder, Phys. Rev. 55, 59 (1939).
[7]States with all quantum numbers the same except for S tune together, but explicit calculation for the He example show that the effect of singlet triplet perturbations should be less than 10 MHz for $L \geq 4$.
[8]M. L. Zimmerman, M. G. Littman, M. Kash, and D. Kleppner, Phys. Rev. A 20, 2251 (1979).
[9]E. U. Condon and G. H. Shortley, *The Theory of Atomic Spectra* (Cambridge University Press, London, 1967).
[10]R. Panock, Ph.D. thesis, MIT, 1979 (unpublished).
[11]A. Corney, *Atomic and Laser Spectroscopy* (Clarendon, Oxford, 1977).
[12]A. Yariv, *Quantum Electronics* (Wiley, New York, 1975).